Neuron, Vol. 27, 385–397, August, 2000, Copyright ©2000 by Cell Press

Three-Dimensional Shape Coding in Inferior Temporal Cortex

Peter Janssen, Rufin Vogels, and Guy A. Orban*
Laboratorium voor Neuro-en Psychofysiologie
KU Leuven Medical School
Campus Gasthuisberg
Herestraat 49
B-3000 Leuven
Belgium

Summary

Neurons in the rostral lower bank of the superior temporal sulcus (TEs), part of the inferior temporal cortex, respond selectively to three-dimensional (3D) shapes. We have investigated how these neurons represent disparity-defined 3D structure. Most neurons were selective for either first-order (disparity gradients) or second-order (disparity curvature) disparities. The latter selectivity proved remarkably vulnerable to disparity discontinuities, such as sharp edges or steps in disparity. The majority of the neurons remained selective for small disparity variations within the stimulus. 3D shape selectivity was preserved when the frontoparallel position or the stimulus size was altered. Thus, in TEs, 3D shape is coded by first- and second-order disparity-selective neurons, which are highly sensitive to spatial variations of disparity.

Introduction

Lesion studies have shown that the inferior temporal cortex (IT) is critical for object recognition (Iwai and Mishkin, 1969; Dean, 1976; Ungerleider and Mishkin, 1982; Weiskrantz and Saunders, 1984). Neurons in the anterior part of IT, area TE, respond selectively to two-dimensional (2D) shape, color, and texture (Gross et al., 1972; Desimone et al., 1984; Tanaka et al., 1991; Komatsu et al., 1992). The shape selectivity of TE neurons can be invariant for changes in size and position and in the visual cue defining the shape (Sato et al., 1980; Schwartz et al., 1983; Sary et al., 1993). Since these neuronal invariances match the invariance of object recognition with respect to size, position, and visual cue, it is believed that small populations of TE neurons represent (views of) objects or parts of objects. Recently, we identified a population of TE neurons (TEs) in the lower bank of the superior temporal sulcus (STS) that respond selectively to three-dimensional (3D) shapes (Janssen et al., 1999b, 2000). The stimuli in these studies were disparity-defined 3D shapes filled with a texture of random dots and smoothly curved in depth. We demonstrated that a large majority of these neurons maintained their 3D shape selectivity when the stimuli were presented at different positions in depth (position-in-depth test), showing that these neurons were not merely responding to absolute disparities (Cumming and Parker, 1999), but to relative disparities (O. M. Thomas et al., 2000, Soc. Neurosci., abstract) or to disparity variations. Therefore, TEs neurons code not only 2D but also 3D object attributes.

The present study was aimed at investigating the representation of 3D shape by TEs neurons. Although zero-order disparity selectivity (e.g., for near or far) was ruled out by the position-in-depth test, it was not clear which higher-order disparity was critical. TEs neurons could be sensitive to a simple disparity gradient at a particular position in the receptive field, i.e., first-order disparity selectivity (e.g., an inclination from far to near), or could code for the variation of the disparity gradient over space, i.e., second-order disparities (e.g., concave versus convex). Higher-order disparity selectivity provides several advantages for the visual system. In contrast to zero-order disparities, first- and second-order disparities are not affected by horizontal and vertical eye misalignments. Moreover, unlike zero-order and first-order disparities, second-order disparities are unaffected by small torsional misalignments of the eyes. Selectivity for zero-order disparity has been demonstrated in both early and dorsal stream visual areas (Poggio and Fischer, 1977; Maunsell and Van Essen, 1983; Poggio et al., 1988; Roy et al., 1992), whereas first-order disparity selectivity has been observed in the caudal intraparietal sulcus (IPS; Shikata et al., 1996; Taira et al., 2000). Thus far, however, no second-order disparity selectivity has been described anywhere in the visual system.

The second aim of the present study was to investigate whether or not these neurons are sensitive enough to represent the small differences in 3D structure typically present in real world objects. Moreover, smoothness is a fundamental property of most natural objects, whereas disparity discontinuities occur frequently at the border of surfaces. We determined whether these neurons required a smoothly curved surface in depth or could tolerate disparity discontinuities, such as sharp edges or steps in disparity. Tolerance to disparity discontinuities would imply that the representation of 3D structure by TEs neurons is relatively coarse. Alternatively, an accurate representation of disparity curvature would require neurons that discriminate between smooth and abrupt changes.

Our previous study demonstrated that TE neurons preserve their 3D shape selectivity over different positions in depth. Here, we also investigate whether or not the selectivity invariances for size and frontoparallel position described for 2D shapes apply to 3D shapes. Invariance for stimulus transformations that leave the overall shape intact is an essential property for neurons that code for shapes or parts of shapes.

Results

We made standard extracellular recordings in three hemispheres of two awake rhesus monkeys. All neurons ($n = 216$) were located in the anterior part of the lower bank of the STS (TEs). A large proportion of the neurons in this area respond selectively to disparity-defined 3D shapes, while being as selective for 2D shape as neurons in lateral TE are (Janssen et al., 2000). 3D shapes filled

*To whom correspondence should be addressed (e-mail: guy.orban@med.kuleuven.ac.be).

with random dot textures were presented while the animals performed a passive fixation task. All neurons were subjected to an initial two-step testing procedure, as described in Janssen et al. (1999b). After a preliminary search test with four different depth profiles (concave, tilted, sinusoidal, and gaussian; see Experimental Procedures), each neuron was tested with two pairs of 3D shapes and monocular presentations to the left or right eye. The members of a pair utilize the same monocular images. A total of 137 of 216 responsive units (63%) showed selectivity for 3D shape. Of these 3D shape–selective neurons, 104 were subsequently tested by presenting the two members of a pair of 3D shapes at five different positions in depth (position-in-depth test).

Position-in-Depth Test

A neuron was classified as responsive to the spatial variation of disparity, i.e., selective for higher-order disparities, if at no position did the response to the nonpreferred 3D shape significantly exceed any response to the preferred 3D shape (80 of 104, or 77% of the neurons tested). A clear example is shown in Figure 1A. The neuron preserved its selectivity at each position in depth (post hoc tests, $p < 0.01$; Kirk, 1968). In this cell, as for the majority of the neurons tested (97 of 104), we measured the horizontal position of only the right eye. No consistent change in the mean eye position (plotted in blue below the peristimulus time histograms [PSTHs] for the extreme positions in depth) occurred during stimulus presentation, although the standard deviation increased slightly. In Figure 2A, we compare for the extreme near and far positions the mean and standard deviation of the right eye position, averaged over all higher-order neurons for which only the position of the right eye was recorded ($n = 78$). We were able to detect a small difference in the mean eye position between far and near presentations (1.3 arcmin), compatible with a small convergence and divergence response for the extreme near and far presentations, respectively. On average, the standard deviation of the eye position difference (in green) did not increase during stimulus presentation, thus excluding the occurrence of convergence and divergence in like proportions, which would leave the mean difference unchanged. The amplitude of the vergence response, however, was negligible compared with the difference between the mean disparity for near and far presentations, which equaled 1 deg. This small vergence response clearly demonstrates the sensitivity of our eye movement recordings. For comparison, Figure 2D shows the time course of the mean and the standard deviation of the right eye position for a genuine vergence response (eye position difference = 0.8 deg) to a target presented at a disparity of ±1 deg.

To exclude the possibility of nonconjugate left eye movements upon stimulus presentation, we measured the horizontal position of both eyes during the position-in-depth test of the 7 (of 104) remaining neurons. The neuron depicted in Figure 1B responded selectively to the concave 3D shape at three positions in depth (positions 1-1′, 2-2′, and 3-3′; post hoc test, $p < 0.01$). At no position in depth did the response to the nonpreferred 3D shape significantly exceed the response to the preferred 3D shape, indicating selectivity for the spatial variation of disparity. Importantly, both the mean and the variability of the eye position difference hardly changed during stimulus presentation. Thus, no vergence eye movements were made upon stimulus presentation. Figures 2C and 2D show the mean eye position difference (left panels) and the mean standard deviation of the eye position difference (right panels) as a function of time for the population of neurons in which

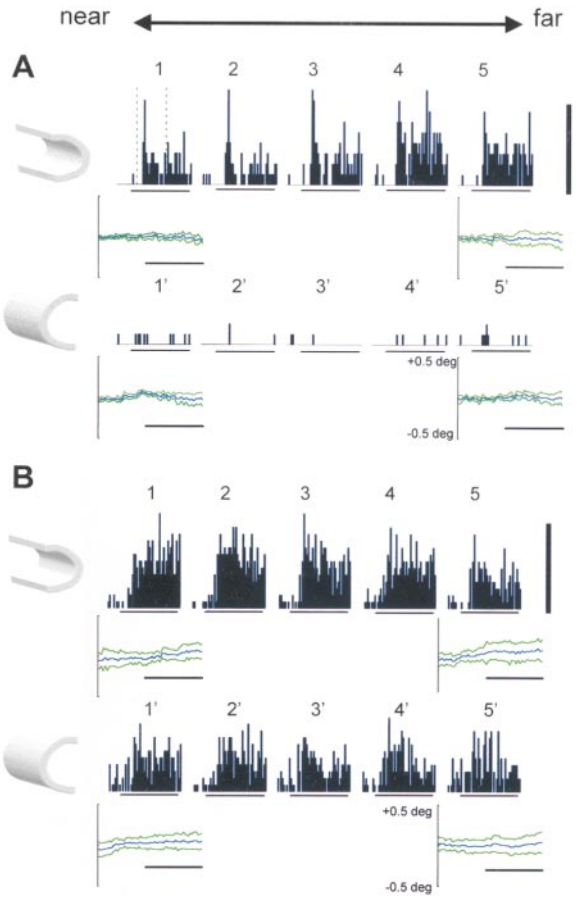

Figure 1. Neuronal Responses in the Position-in-Depth Test

In both parts, the top row shows the PSTHs of the preferred 3D shape at five positions in depth (1–5) ranging from −0.5 deg (near) to +0.5 deg (far); the bottom row shows the responses to the nonpreferred 3D shape (1′–5′). Bin width is 20 ms. The perceived 3D structure is illustrated on the left. This illustration does not show the actual borders of the stimulus. The observer is to the left. Horizontal bars indicate the duration of stimulus presentation.

(A) TEs neuron showing invariance of the 3D shape preference at all positions in depth (post hoc tests, $p < 0.01$). Below the histograms, the mean (in black) ± the standard deviation (in green) of the smoothed right eye position (five points running average, 25 ms) are plotted as a function of time for the extreme positions in depth. The scale of the eye position traces is ±0.5 deg, and the vertical calibration bar indicates 80 spikes/s. Vertical dashed lines in 1 indicate the response analysis window.

(B) TEs neuron showing partial invariance of 3D shape preference over different positions in depth. The net response to the preferred 3D shape differed significantly from that to the nonpreferred 3D shape at positions 1, 2, and 3 (post hoc test, $p < 0.01$). The mean smoothed (five points running average) difference between the horizontal positions of the left and right eyes (in black) is plotted below the histograms for the extreme positions in depth. The green traces represent the mean ± the standard deviation of the eye position difference. The vertical calibration bar on the right indicates 50 spikes/s.

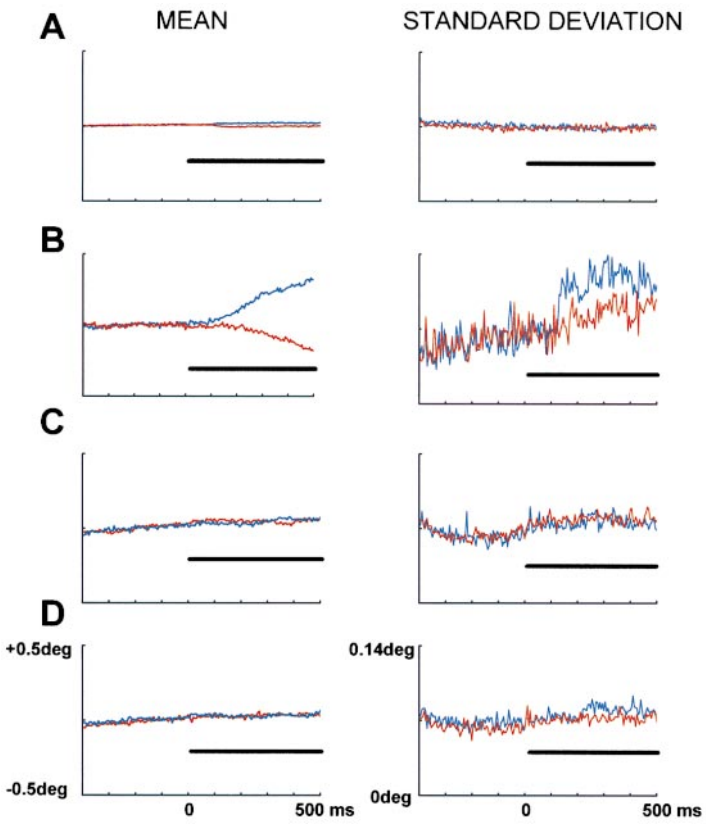

Figure 2. Eye Movement Recordings in the Position-in-Depth Test

(A) Mean right eye position (left panel) and mean standard deviation of the eye position (right panel) for the extreme near (red) and far (blue) stimulus presentations (n = 78 higher-order neurons).

(B) Mean right eye position (left panel) and standard deviation of the eye position (right panel) for a genuine vergence response on a target presented at 1 deg near (red) and far (blue) disparity (n = 20 trials).

(C) Mean difference in the position of the left and right eyes (left panel) and mean standard deviation of the difference in eye position (right panel) for the extreme near (red) and far (blue) presentations of a concave 3D shape (n = 7 neurons).

(D) As in (C), but for a convex 3D shape.

the positions of both eyes were recorded (n = 7, 2 of which were higher-order neurons). Clearly, neither the mean nor the standard deviation was influenced by the position in depth of the stimulus (blue, far; red, near). Taken together, the analysis of the two types of eye movement recordings demonstrates convincingly that the preserved 3D shape preference at different positions in depth is not a result of vergence eye movements, confirming our earlier report (Janssen et al., 1999b).

In contrast to the neurons in Figure 1, 24 of 104 neurons tested reversed their selectivity in the position-in-depth test. An example neuron is shown in Figure 3. In the initial test with monocular controls, the neuron responded selectively to the convex 3D shape (replicated in the position-in-depth test at positions 3 and 3′ in Figure 3A). However, presentation of the "preferred" depth profile behind the plane of fixation evoked no activity (positions 4 and 5), whereas presenting the "nonpreferred" 3D shape in front of the plane of fixation (position 1′) resulted in significant responses (analysis of variance [ANOVA], position × stimulus interaction: $F[4, 70] = 18.14$, $p < 0.0001$). Apparently, the 3D shape selectivity of this neuron resulted from a relative preference for near disparities, which were present in the central part of the original convex stimulus but absent in the original concave 3D shape. This interpretation was confirmed by presenting a flat shape at five positions in depth (Figure 3B). Only zero and near disparities were effective in driving the neuron (ANOVA, $F[5, 44] = 90.9$, $p < 0.0001$). Note that the neuron did not respond to the 3D shape in condition 2′, even though the stimulus consisted entirely of zero and near disparities. The activation of the neuron required a surface of a certain spatial extent, not merely the tip of the 3D shape, as in conditions 4 and 2′, lying within the preferred disparity range. Because the selectivity of the neuron reversed in the position-in-depth test (compare position 5 to position 1′), this neuron was classified as zero-order disparity selective.

For each neuron, we computed a selectivity index (see Experimental Procedures) for the middle position (SI_m, position 3, in Figure 3A), and a selectivity index comparing the smallest response with the preferred 3D shape and the largest response with the nonpreferred 3D shape (SI_w, position 5, compared with position 1′ in Figure 3A; a negative index indicates a larger response to the nonpreferred 3D shape). Thus, the SI_w provides a worst case measure of the 3D shape selectivity in the position-in-depth test. Figure 3C shows a scatter plot of the two selectivity indices for both zero-order neurons (in which, by definition, the SI_w was significantly less than zero) and higher-order neurons. The SI_w for higher-order neurons never exceeded −0.33, whereas for zero-order neurons, the index was always smaller than −0.33. In contrast to our previous study (Janssen et al., 1999b), a substantial proportion of the higher-order neurons (27%) remained selective at all five positions in depth (e.g., the neuron in Figure 1A). Post hoc tests computed at each position in depth revealed that on average, the selectivity for 3D shape was significant at four of five positions.

The data presented below were obtained only with higher-order disparity-selective neurons (i.e., neurons responsive to the spatial variation of disparity). Neurons responsive to mere zero-order disparities are not discussed further.

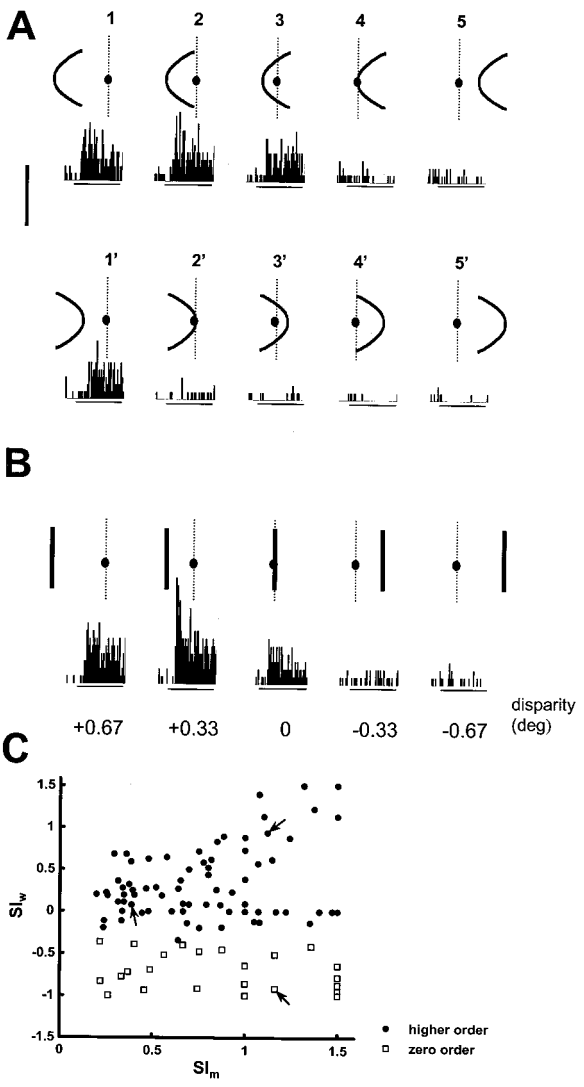

Figure 3. Zero-Order Disparity Selectivity

(A and B) Responses of a zero-order disparity-selective neuron to a pair of 3D shapes (A) and a flat shape (B) in the position-in-depth test. The icons above the PSTHs illustrate the position in depth of the stimulus, with reference to the plane of fixation (dotted line) and the fixation point (near is to the left, far is to the right). In (B), the disparity range was extended to cover the whole range in the curved shapes. The vertical calibration bar indicates 60 spikes/s. Same conventions as in Figure 1.

(C) Scatter plot of the selectivity index at the worst position (SI_w) plotted as a function of the selectivity index middle position (SI_m). Open squares represent zero-order disparity-selective neurons, closed circles higher-order disparity-selective neurons. The arrows indicate the neurons depicted in Figure 1A (top right), Figure 1B (left middle), and Figure 3A (bottom right).

Selectivity for Small Differences in 3D Structure

Sixty-four higher-order neurons were tested with different disparity magnitudes, i.e., the range of disparity contained in the stimulus. The smallest magnitudes equaled 0.06 deg for the tilted and the sinusoidal depth profiles and 0.03 deg for the concave and the Gaussian depth profiles. Examples of the monocular images in this test are illustrated above the PSTHs in Figure 4. The neuron illustrated in Figure 4A responded strongly and selectively to the convex 3D shape with a large magnitude (1.3 and 0.65 deg). As the magnitude decreased, the response of the unit declined monotonically (ANOVA, $F[5, 96] = 35.9$, $p < 0.0001$). However, even for the lowest magnitude tested (0.03 deg), the neuron responded significantly better to the convex 3D shape than to the concave 3D shape (post hoc test, $p < 0.0001$). Clearly, the neuron was selective for small differences in 3D structure but was also sensitive to the magnitude of the disparity variation. Figure 4B shows a neuron in which the high disparity magnitudes elicited relatively weak but selective responses to the concave 3D shape. As the magnitude decreased, the response rate of the neuron actually increased (ANOVA, $F[5, 43] = 28.01$, $p < 0.0001$), reaching a maximum at 0.16 deg (post hoc test comparing the 0.16 and 0.03 magnitudes, $p < 0.001$). Even more clearly than in Figure 4A, 3D shape selectivity was preserved for the lowest disparity magnitude (post hoc test, $p < 0.0001$).

Both neurons in Figure 4 illustrate the general finding that TEs neurons exhibit a remarkable selectivity for small differences in 3D structure. Overall, 66% of the neurons tested with a magnitude of 0.03 deg (29 of 44 neurons) remained 3D shape selective. At a viewing distance of 86 cm, a disparity magnitude of 0.03 deg corresponds to a horizontal separation of the monocular images of 0.5 mm and (for an interocular distance of 4 cm, as with our monkeys) to a variation in depth of 1 cm along the 8.4 cm vertical axis. The number of neurons remaining selective for the lowest magnitudes depended on the preferred 3D shape. Even though the disparity magnitude was smaller for the concave and the Gaussian 3D shapes (0.03 deg) than for the tilted depth profile (0.06 deg), neurons responsive to the former stimuli were significantly more frequently selective for the smallest magnitudes tested (15 of 24, or 63%, for the concave and 14 of 20, or 70%, for the Gaussian 3D shape) than were neurons responsive to the tilted depth profile (2 of 14, or 14%, Kruskal-Wallis median test, $p < 0.001$).

Based on statistical criteria (see Experimental Procedures), we classified the neurons into one of three classes (Figure 5A). The most frequently encountered type of neuron (46%) showed monotonically decreasing response rates for decreasing disparity magnitudes, as was the case for the neuron in Figure 4A; 37% of the neurons tested were tuned for a specific disparity magnitude. Although we searched for responsive neurons using relatively large magnitudes (0.65 deg), we discovered neurons tuned to every disparity magnitude in the test. A third type of neuron ("broad band," 17%) was not significantly affected by reductions in disparity magnitude.

Most 3D shape–selective neurons were particularly sensitive to the direction (or the sign) of the disparity magnitude. Figure 5B plots the mean net response for the entire population of neurons tested as a function of the disparity magnitude. Since all tuned responses average out, only the decline in response rate remains. However, it is evident that the greatest difference between the responses of two consecutive magnitudes occurs between $+1$ and -1, i.e., where the 3D structure changed from convex to concave (or vice versa). In this transition, the difference in disparity magnitude was very small (0.06 deg or 0.12 deg), yet the difference in normalized response averaged 42% of the response to the optimal magnitude, which was significantly greater than

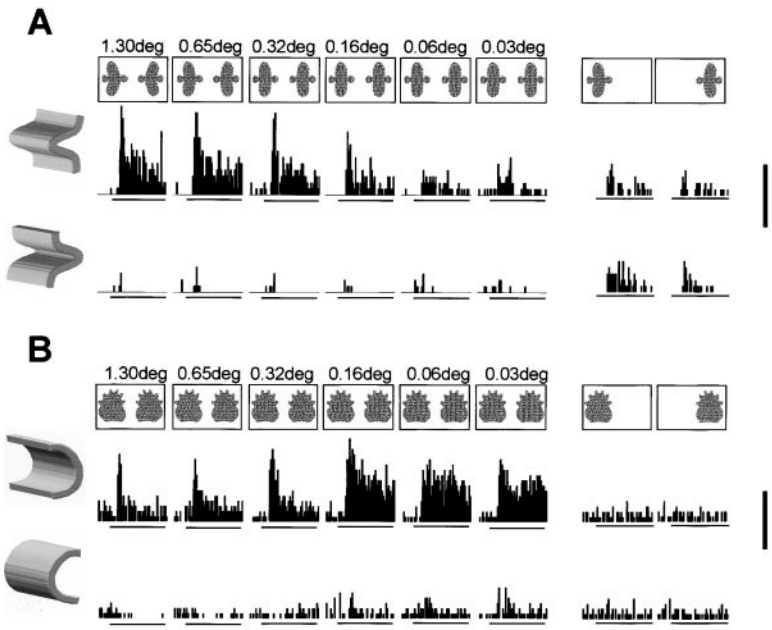

Figure 4. Neuronal Responses in the Sensitivity Test

The monocular images of the preferred 3D shape are illustrated above the PSTHs. For the nonpreferred 3D shape, these images were interchanged between the eyes. PSTHs for the preferred 3D shape are plotted in the top row, those for the nonpreferred 3D shape in the lower row. The two histograms on the right show the monocular responses of the neurons for the 0.65 deg disparity magnitude.

(A) TEs neuron showing monotonically decreasing responses for decreasing disparity magnitudes. The vertical calibration bar on the right indicates 40 spikes/s.

(B) TEs neuron tuned to the 0.16 deg disparity magnitude. The vertical calibration bar indicates 50 spikes/s.

for any of the other, much larger transitions between consecutive magnitudes (post hoc tests, $p < 0.0001$).

Twenty-five neurons were also tested with a flat shape at zero disparity, lying halfway between the 3D structures of the preferred and the nonpreferred 3D shapes at the lowest disparity magnitude. The mean normalized response to the flat shape (33% of the response to the optimal disparity magnitude) differed significantly from the response to the preferred 3D shape with the smallest disparity magnitude (54%, post hoc test, $p < 0.001$) but was similar to that of the nonpreferred 3D shape (23%, post hoc test, ns).

First- and Second-Order Disparity Selectivity

We investigated whether 3D shape–selective TEs neurons are selective for first- or second-order disparity variations. Selectivity for first-order disparities would imply the coding of a linear spatial change in disparity (disparity gradient), while second-order disparity selectivity would mean that the neurons code the change of the disparity gradient over the surface of the shape (disparity curvature; Figure 6A). A second goal of this experiment was to determine to what extent a smoothly curved surface is necessary for 3D shape selectivity. Thus, in the disparity order test, each neuron was tested with the original preferred and nonpreferred 3D shapes, first-order stimuli, and various approximations of these shapes. The first-order stimuli consisted of least-squares approximations of the upper or lower parts of the original 3D shape, which were extrapolated over the entire surface of the shape. The linear approximation of the second-order stimuli was a least-squares approximation of the whole 3D shape and consisted of two connected parts of first-order disparity. Notice the subtle difference in 3D structure between the original 3D shape and its linear approximation. The disparity gradients of the upper and lower parts of the linear approximation are very similar to those of the original 3D shape (Figure 6B, left panel). Therefore, the main difference between these two 3D shapes resides in the apex of the linear approximation. Finally, the three or four discrete approximations each contained one or two steps in disparity, equal to the disparity magnitude in the original 3D shape, at different positions along the vertical axis (Figures 6B and 6C).

Figure 7A shows a neuron selective for a disparity gradient. The linear approximation of the tilted 3D shape corresponds to a disparity gradient. Clearly, the selectivity of the neuron was almost identical for the two 3D pairs (post hoc test, ns), and even the discrete approximations resulted in significant selectivity (post hoc test, $p < 0.01$). Overall, 11 of 45 neurons tested (24%) were as selective to the linear change of disparity as to the original pair, i.e., were first-order disparity selective. Since the search stimuli all contained second-order disparities, and half of them contained opposing first-order disparities (e.g., the upper and lower part of the concave 3D shape; Figure 4A), this proportion is likely to be an underestimation of the real proportion of first-order disparity-selective neurons. Figure 8A plots the absolute response difference for the first-order stimuli against the response difference for the original 3D shape pair. First-order neurons cluster along the diagonal. Note that a large proportion of the second-order neurons displayed no selectivity for the first-order stimuli, whereas others did show first-order selectivity. Moreover, some second-order neurons responded strongly—though less selectively—to the first-order stimuli (Figure 8B).

Of the higher-order neurons, 76% (34 of 45) were significantly more selective for the original 3D shapes than for the first-order stimuli. These second-order neurons required a spatial variation in the disparity gradient. The largest subpopulation (16 of 34, or 47%) responded significantly more strongly to the original 3D shape than to its linear approximation, i.e., were selective for a smoothly curved surface in depth. Since these neurons were apparently sensitive to the second spatial derivative of disparity over position (i.e., disparity curvature), they are referred to as curvature neurons. Figure 7B shows an example of a curvature neuron responding strongly and selectively to the concave 3D shape. The

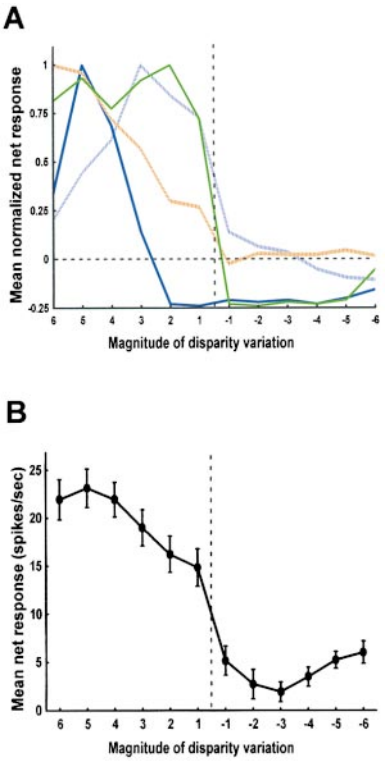

Figure 5. Summary of the Sensitivity Test

(A) Examples of the different types of TEs neurons. The mean normalized net response is plotted to the 12 disparity magnitudes in the test (classes 6 to 1: preferred 3D shape, decreasing magnitudes; classes −1 to −6: nonpreferred 3D shape, increasing magnitudes). Green, broad band neuron; blue, neurons tuned to a high disparity magnitude (solid line) and to a lower magnitude (dotted line); red, monotonic neuron. The dotted lines represent the neurons illustrated in Figures 4A (red) and 4B (blue).

(B) Mean (±SE) net response to the 12 disparity magnitudes in the test for the population of neurons (n = 64). Note the sharp decrease in the average response when the disparity variation changed sign (between classes 1 and −1).

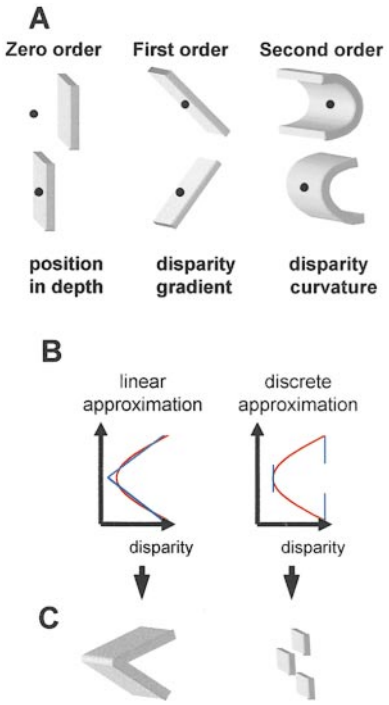

Figure 6. Schematic Illustrations of the Stimuli in the Disparity Order Test

(A) Zero-order disparities (left panel) refer to position in depth, and first-order disparities (middle panel) are linear variations of disparity, whereas second-order disparities (right panel) describe the spatial variation of the disparity gradient.

(B) The variation of disparity over the vertical position in the original 3D shape (red), in the linear approximation (blue, left panel), and in one of the discrete approximations (blue, right panel).

(C) Illustrations of the perceived 3D structure of the linear approximation (left) and one of the discrete approximations (right).

linear approximation of the original 3D shape evoked a much weaker response (mean net response = 7.3 spikes/s compared with 32.8 spikes/s for the original 3D shape, post hoc test, $p < 0.0001$), whereas the discrete and first-order approximations did not activate the neuron at all.

The second largest group (12 of 34, or 35%) consisted of neurons that were equally responsive for the linear approximation and the original 3D shape. These cells required second-order disparities, and did tolerate the disparity discontinuity at the edge of the shape but not discrete steps in disparity. We refer to these cells as wedge neurons. For the neuron in Figure 7C, the linear approximation elicited a response almost identical to that of the original, smoothly curved 3D shape (mean net response = 70.3 spikes/s and 72.1 spikes/s, respectively, post hoc test, ns). Responses to the discrete approximations of preferred and nonpreferred 3D shape did not differ significantly, whereas the first-order approximations yielded only weak and nonselective responses (post hoc test, ns). Again, second-order disparities were critical for 3D shape selectivity, but the linear approximation was as effective as the smoothly curved 3D shape was.

Figure 8D plots the response to the linear approximation against the response to the original preferred 3D shape for wedge neurons (located near the diagonal) and curvature neurons. In Figure 8C, the response difference for the linear approximations is shown as a function of the response difference between preferred and nonpreferred original, curved 3D shape. Curvature neurons responded on average two and a half times less to the linear approximation than to the original 3D shape (for wedge neurons, this ratio equaled 1/1.05). Half of the curvature neurons (8 of 15) displayed no significant selectivity for the linear approximation (bottom symbols in Figure 8C). Curvature neurons began signaling differences between the 3D structures of the original and the linear approximation early in the response. These differences reached significance at 100 ms after stimulus onset and 20 ms after response onset (post hoc test, $p < 0.05$). Given the high degree of similarity between the gradients of the linear approximation and the original 3D shape (Figure 6B), it is unlikely that other values of disparity gradients would have produced more similar responses to linear approximations and original, curved surfaces.

For only six neurons (18%), the discrete approximations evoked a selectivity comparable to the original

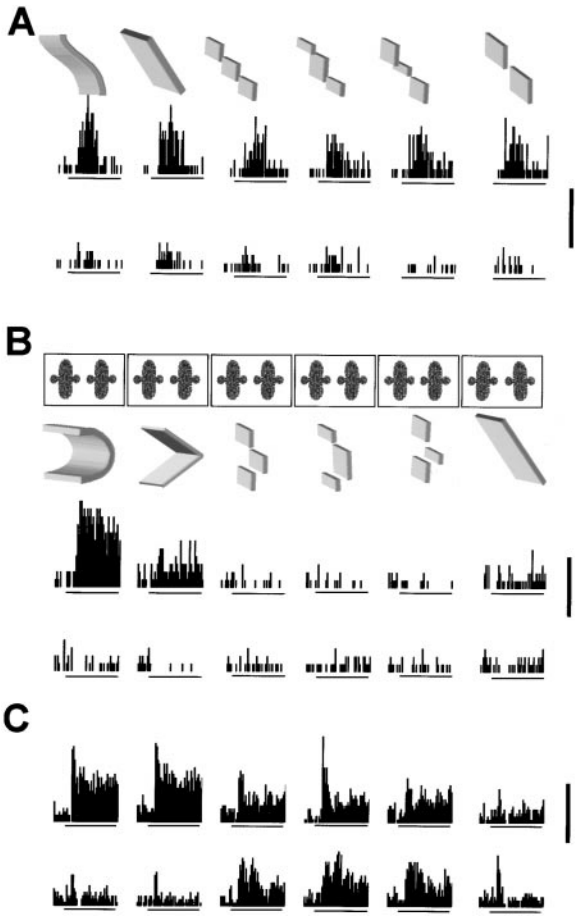

Figure 7. Neuronal Responses in the Disparity Order Test

In each part, the top row of PSTHs shows the responses to the preferred 3D shape, the bottom row the responses to the nonpreferred 3D shape. The perceived 3D structure of the preferred 3D shape and its approximations are illustrated above the PSTHs. The monocular images of the 3D shapes in (B) and (C) are shown in (B). Same conventions as in Figure 1.

(A) Responses of a first-order disparity-selective neuron in the disparity order test. The vertical calibration bar indicates 30 spikes/s.

(B) Example of a second-order curvature neuron. The vertical calibration bar indicates 30 spikes/s.

(C) Example of a second-order wedge neuron. The vertical calibration bar indicates 90 spikes/s.

3D shape. In these discrete neurons, the interaction between stimulus type and approximation (original, linear, and discrete approximation) was not significant. In Figure 8E, the response differences for the discrete approximation yielding the largest response are plotted against the response differences between preferred and nonpreferred original, curved 3D shape. As expected, discrete neurons fall above the diagonal, whereas curvature and wedge neurons are located under the diagonal. Many neurons showed no selectivity for the discrete approximations (response difference close to zero). In three neurons, the 3D shape selectivity even reversed for the discrete approximations (arrowheads). The peripheral segments of the nonpreferred discrete approximation appeared at a disparity for which the neurons were tuned, as confirmed by presenting flat shapes at different positions in depth. In Figure 8F, the response to the best discrete approximation is plotted against the response to the original 3D shape. Note that some wedge and curvature neurons gave similar responses to discrete and smoothly curved 3D shapes, as did the majority of the discrete neurons.

To exclude the possibility that an absence of selectivity for discrete approximations was a result of a nonoptimal disparity magnitude, we repeated the same test with a disparity magnitude of 0.06 deg for five neurons that had shown significant 3D shape selectivity at the smallest magnitude tested in the sensitivity test (0.03 deg). The 0.06 deg magnitude is the smallest magnitude for which the 3D structure of the original shape differs from that of its approximations. (A magnitude of 0.03 deg yields "discrete" stimuli for all conditions, since the disparity range equals only one pixel.) Surprisingly, these five neurons showed no selectivity for any of the discrete approximations (mean response difference = 2.8 spikes/s, Wilcoxon matched pairs test, ns), in contrast to the large differences in the responses to the 0.06 deg magnitude of the smooth 3D shape pair (mean response difference = 29.7 spikes/s, Wilcoxon matched pairs test, $p < 0.05$). This result shows that a nonoptimal disparity step size could not account for the poor selectivity for discrete stimuli. In addition, TEs neurons are not only sensitive for the direction of the disparity variation; they are also remarkably sensitive to the size of a discrete step in disparity.

We noted a distinction among the different subpopulations of higher-order neurons in the degree of stimulus selectivity for the original 3D shape. Although the group $\times$ stimulus interaction failed to reach significance ($F[3, 41] = 2.18$, $p = 0.05$), curvature neurons tended to be more selective than all other types of neurons. The ratio of the mean net response to preferred versus nonpreferred 3D shape equaled 33.6 for the curvature neurons compared with 4.4, 3.0, and 4.6 for wedge, discrete, and first-order neurons, respectively.

Invariance for Position in the Frontoparallel Plane

Twenty-five neurons (five first-order and twenty second-order neurons) were tested with the original preferred and nonpreferred 3D shapes presented foveally and at four eccentric positions in the frontoparallel plane (ipsilateral, contralateral, up, down; eccentricity, 2.3 deg). Figure 9A shows a neuron that is selective at every position tested (post hoc tests, $p < 0.001$). Although the response of the neuron varied with the frontoparallel position (the net response was on average reduced by 68% in the eccentric presentations compared with the center position), its preference for 3D shape remained invariant, illustrating the dissociation between preference and response levels typical of TE neurons.

For every neuron tested, we ranked the five positions according to the magnitude of the net response to the preferred 3D shape (defined at the best position). Figure 9B shows the mean net responses to preferred and nonpreferred 3D shapes as a function of position rank. While eccentric presentations affected the mean response (average reduction of 30% compared with the center position, which was the best position in 56% of the neurons), 3D shape preference was preserved at the population level, even at the worst position (ANOVA on the worst position responses, $F[1, 24] = 21.6$, $p < 0.001$). Furthermore, ten neurons (40%) were selective at every eccentric position tested. No correlation existed between the order of disparity selectivity and the number

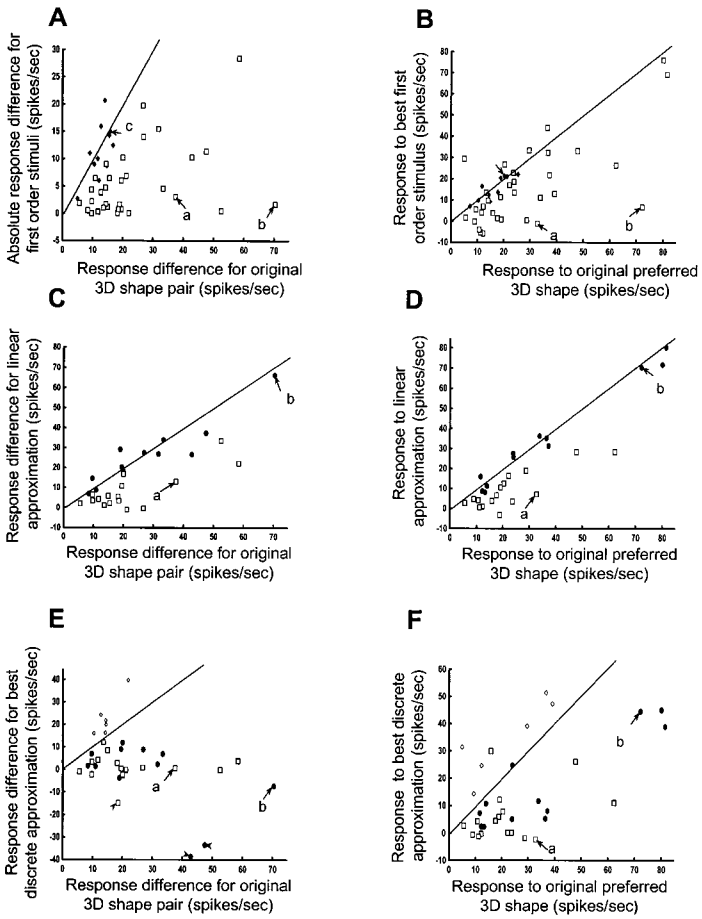

Figure 8. Scatter Plots of the Responses in the Disparity Order Test

Arrows indicate the neurons shown in Figure 7 ("a," curvature neuron; "b," wedge neuron; "c," first-order neuron).

(A) Absolute response difference for the first-order stimuli plotted as a function of the response difference for the original 3D shape pair, for first- (closed diamonds) and second-order (open squares) neurons.

(B) Response to the best first-order stimulus plotted as a function of the response to the original preferred 3D shape. Same conventions as in (A).

(C) Response difference for the linear approximations as a function of the response difference for the original 3D shape pair for curvature (open squares) and wedge (closed circles) neurons.

(D) Response to the linear approximation as a function of the response to the original 3D shape. Same conventions as in (C).

(E) Response difference for the best (largest response) discrete approximation as a function of the response difference for the original 3D shape pair, for discrete (open diamonds), wedge (closed circles), and curvature (open squares) neurons. Arrowheads indicate the neurons that reversed their selectivity for the discrete approximations.

(F) Response to the best discrete approximation plotted as a function of the response to the preferred 3D shape. Same conventions as in (E).

of positions showing significant 3D shape selectivity or the degree of response reduction for parafoveal presentations.

Invariance for Changes in Size

The primary purpose of this test was to determine the extent to which 3D shape–selective neurons remain selective when the size of the stimulus is altered, as reported for 2D shape selectivity (Sato et al., 1980; Schwartz et al., 1983; Ito et al., 1995). The second purpose was to investigate whether TEs neurons are sensitive to disparity curvature as such. In the sensitivity test, we observed that many TEs neurons were sensitive to the disparity magnitude. In that stimulus, the amount of protrusion or involution (i.e., the disparity difference between the border and the central part of the shape) and disparity curvature (the rate of the disparity change over space) covaried. In the size test, we obtained a range of protrusions/involutions for a given disparity curvature by manipulating the size of the stimulus, allowing the independent measurement of curvature and protrusion/involution effects. The left panel of Figure 10A illustrates the size variation (ranging from 8.4 to 2.8 deg). On the right, we plotted the variation of disparity over vertical position for the two largest sizes. Disparity varied with vertical position according to a quadratic function, implying that the second spatial derivative is constant. The same three functions relating disparity to position (denoted "a," "b," and "c" in Figure 10A) were utilized for every size, which resulted in a 3-fold variation in disparity curvature for every size. For neurons tuned to disparity curvature, a shift in the curvature tuning for a different size would indicate that the neurons respond to the amount of protrusion. In contrast, the same curvature would remain optimal in neurons sensitive to disparity curvature.

Figure 10B illustrates a neuron showing invariance of the 3D shape preference for changes in size (post hoc tests comparing preferred to nonpreferred 3D shape, $p < 0.0001$ for every combination of size and curvature). The response to the preferred 3D shape, however, was significantly affected by both the size manipulation and the variation in disparity curvature ($F [2, 198] = 118.3$, $p < 0.0001$, and $F [2, 198] = 19.0$, $p < 0.0001$, respectively). The neuron preferred the two largest sizes and the smallest curvature, although it is noteworthy that the interaction between size and curvature was not significant ($F [4, 198] = 1.95$, ns). Since the response curve was monotonic, no shift of the preferred curvature could be detected.

In all neurons tested ($n = 14$), size showed significant effects. In the averaged population responses, the 2.8 deg diameter stimulus was the least effective 3D shape (significant interaction between stimulus and size, $F[2, 264] = 3.65$, $p < 0.05$). In eight neurons (57%), disparity curvature showed a significant main effect. Figure 10C plots the mean net responses of these neurons, ranked according to preferred size (from left to right). These neurons generally preferred the smallest curvature, and

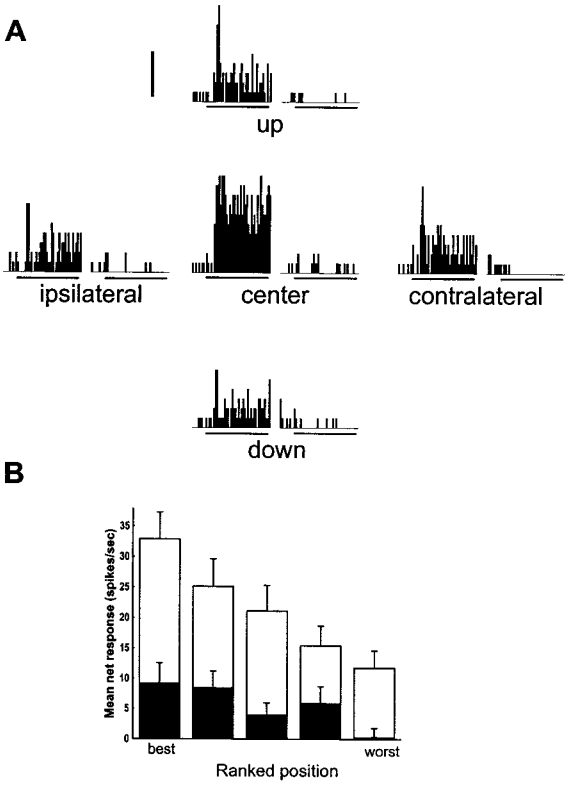

Figure 9. Frontoparallel Position Test

(A) Example of a TEs neuron showing 3D shape preference invariance for different positions in the frontoparallel plane. The vertical calibration bar indicates 40 spikes/s. Same conventions as in Figure 1.

(B) Average net responses (+SE) to preferred (open bars) and nonpreferred (closed bars) 3D shape, defined at the best position, for five positions ranked according to the magnitude of the net response (n = 25).

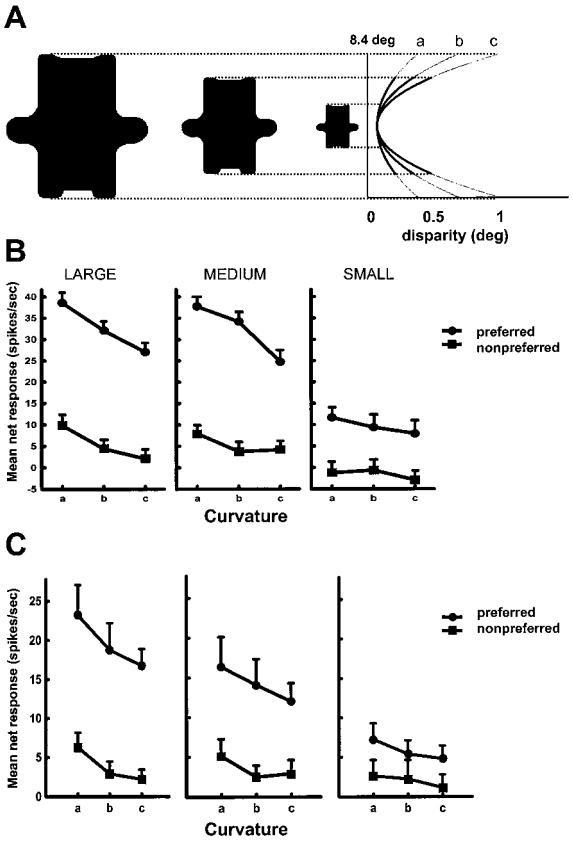

Figure 10. Stimuli and Neuronal Responses in the Size Test

(A) On the left, the variation in size is illustrated for one of the shapes. The middle size was the standard size. On the right, the three quadratic functions relating disparity to the vertical position (denoted "a," "b," and "c") are shown. Each size was presented with each of the disparity curvatures.

(B) Example neuron showing invariance of 3D shape preference for the different sizes in the test. The neuron preferred the smallest curvature and the two largest sizes.

(C) Average net responses (+SE) of all neurons in which disparity curvature showed a significant effect (n = 8), ranked according to preferred size (from left to right).

this preference was similar for every size tested. Only one of the six remaining neurons showed a significant interaction between size and curvature, caused by an absence of responses to the smallest size. The absence of tuned responses to the middle disparity curvature, however, prevented us from drawing any firm conclusions about the relative contributions of protrusion/involution and curvature to the neuronal selectivity.

Discussion

The present study investigated how TEs neurons process the 3D structure of shapes. We found that the neural representation of 3D shape is highly sensitive to small disparity variations and that the population of neurons displays zero-, first-, and second-order disparity selectivity, including selectivity for disparity curvature. As demonstrated for 2D shape (Schwartz et al., 1983; Ito et al., 1995), the preference for 3D shape (but not the response) generally remains invariant over different positions in the frontoparallel plane and over changes in size.

The fact that half of the neurons remained selective for the smallest disparity magnitude tested demonstrates a sensitivity sufficient to represent the 3D structure of many real world objects. Moreover, TEs neurons were much more affected by a change in the direction of curvature (e.g., from concave to convex) than by any other transition between consecutive magnitudes. The neural code is not strictly qualitative, however, since a sizeable proportion of the neurons were tuned for a particular disparity magnitude. It seems that the magnitude of the disparity variation is represented in a distributed code with a distinct sensitivity for the direction of the disparity magnitude, which can be regarded as a nonaccidental shape property (Lowe, 1986).

This study provides the first evidence for the existence of second-order disparity-selective neurons in the visual system. Tuning for position in depth has been described in both early visual (Poggio and Fischer, 1977; Burkhalter and Van Essen, 1986; Poggio et al., 1988) and dorsal stream areas (Maunsell and Van Essen, 1983; Roy et al., 1992). Shikata et al. (1996) and Taira et al. (2000) reported that neurons in the caudal bank of the IPS respond selectively to the disparity-defined orientation in depth

of a square plate, which could represent first-order disparity selectivity. We demonstrated that neurons in a high-level area of the ventral visual stream are selective for second-order disparities. Howard and Rogers (1995) have already speculated that the visual system may extract second-order disparities to benefit from the fact that the local value of disparity curvature remains approximately constant for changes in viewing distance. It should be noted that the exact proportions of the classes of higher-order neurons may have been different for a different set of stimuli. Also, these classes must not be viewed as discrete categories, but more as a continuum from the relatively coarse 3D shape selectivity of discrete neurons to the refined selectivity of curvature neurons. Our data suggest that the neuronal representation of disparity curvature may be finer than that of first-order disparities. In the sensitivity test, neurons responsive to the tilted 3D shape (which contained only a single first-order component; Figure 7A, top row) were significantly less often selective for the smallest magnitudes than were neurons responsive to the convex/concave or Gaussian depth profile. Similarly, the degree of stimulus selectivity in the disparity order test was smaller for first-order neurons than for curvature neurons (Figure 8A).

The lower bank of the STS contained neurons selective for second-, first-, and zero-order disparities. Lower-order neurons are likely to provide the antecedent computations necessary for second-order selectivity. The afferents carrying this selectivity could originate either from earlier ventral areas (TEO or V4) or from the caudal bank of the IPS, which projects directly to the lower bank of the STS (Seltzer and Pandya, 1978; Baizer et al., 1991). We cannot decide whether our zero-order neurons were selective for absolute disparities, as in V1 (Cumming and Parker, 1999), or for relative disparities. However, neurons selective for the discrete approximations in the disparity order test merely required a disparity difference between the central and the peripheral segments of the stimulus. Since the preference for 3D shape was preserved at different positions in depth, these neurons were responsive to the relative disparity in the stimulus. All other second-order neurons did not tolerate large steps in disparity. Note that, due to limitations in display resolution, even the smoothly curved 3D shapes were composed of discrete segments separated in depth by a disparity of 0.03 deg, which implies that these neurons do tolerate small steps in disparity. Also, a small number of higher-order neurons responded as well to discrete approximations as to the original 3D shape, although their 3D shape selectivity was significantly reduced for discrete, compared with linear, approximations and the original 3D shape pair. These neurons only signal differences in 3D structure for continuous surfaces (Figure 8F).

The results from the frontoparallel position test demonstrate that 3D shape preference can be preserved over frontoparallel changes in position, as described for 2D shape selectivity. However, the degree of response invariance for disparity-defined 3D shapes appeared to be less pronounced than that for 2D shapes. Horizontal displacement by 2.3 deg resulted in an average decrease of 30% in response, whereas for 2D features, the decrease at 6.5 deg eccentricity averaged only 25% (Vogels, 1999). This result suggests that selectivity for disparity-defined 3D shape depends more upon foveal input than does selectivity for 2D shape, which is not surprising given the impressive selectivity for small differences in 3D structure displayed by these neurons. It is important to note, however, that the position invariance of 3D shape preference in the frontoparallel plane provides an additional argument against the possibility that TEs neurons are merely extracting a change in disparity at a particular position in the receptive field.

In the size test, the average response to the smallest size (2.8 deg) was reduced by 40% compared with the optimal size, which was only twice as large in vertical extent. This size effect was very consistent for the relatively small number of neurons tested. It contrasts markedly with the size invariance reported for 2D shape. Ito et al. (1995) found that 21% of the lateral TE neurons showed a decrease of $<$50% over a 32-fold size range (from 1.6 to 52.2 deg). This size dependency suggests that 3D shape selectivity requires a minimal spatial extent over which the disparity variation is computed. It is tempting to speculate that neurons in earlier visual areas would be less sensitive to second-order disparities, since the size of their receptive fields—especially the foveal ones—is much smaller than in TE (Gatass et al., 1988). Overall, the basic stimulus invariances for 2D shape have been replicated for 3D shape, but the extraction of disparity variations imposes specific constraints on the degree of invariance that can be obtained.

The neuronal selectivity for disparity-defined 3D structure was remarkably analogous to the performance of human subjects in tasks requiring the discrimination of 3D structure. Note that stereothresholds for monkey and human observers have been found to be very similar (Harwerth and Boltz, 1979; Harwerth et al., 1995). Human observers are very accurate in discriminating the direction (or the sign) of surface curvature. Bradshaw and Rogers (1993, Perception [Suppl.], abstract) reported that the peak-to-trough thresholds for the detection of disparity-defined corrugations could be as low as 2 arcs for foveal presentations. Two surfaces can be reliably discriminated when the curvature difference is only 5% of the reference disparity curvature of 3 arcmin/deg^2 (Rogers and Cagenello, 1989). Although impressive, these thresholds (0.15 arcmin/deg^2) are clearly higher than those for discrimination of direction of curvature (0.02 arcmin/deg^2). We observed a striking parallel with these psychophysical data, in that TEs neurons were much more strongly affected by a change in the direction of curvature than by any other transition between two consecutive magnitudes. In addition, constant disparity gradients yield only weak apparent depth perception that can be easily overruled by conflicting monocular depth cues (Stevens and Brookes, 1988). The same phenomenon was observed at the single cell level, since the selectivity for first-order stimuli appeared to be coarser than for second-order disparities.

Norman et al. (1991) showed that human observers are very accurate in discriminating a (discontinuous) triangular wave (similar to our linear approximation) from a smoothly curved surface with the same overall shape, not unlike the selectivity for smooth stereoscopic surfaces we observed at the neuronal level (curvature neurons). These authors suggested that the primary difference between the two stimuli lies in their second spatial derivatives, which are either undefined at the apex or zero everywhere else for the triangle wave, as opposed to the smooth surface, which is differentiable everywhere.

The effects of stimulus size and frontoparallel position

on the neuronal response once again match the available psychophysical data. For human observers, the thresholds for the discrimination of disparity-defined corrugations increase by a factor of 5 at an eccentricity of 3.5 deg compared with foveal presentation (Prince and Rogers, 1998). Moreover, the thresholds for the discrimination of the direction of curvature are ten times higher for a stimulus diameter of 2.66 deg compared with one of 20 deg (Howard and Rogers, 1995).

An influential theory on stereopsis proposes that the coding of surface structure is directly associated with the differential structure of the disparity field (Koenderink and van Doorn, 1976; Stevens and Brookes, 1988; Rogers and Cagenello, 1989). In line with this theory, the present study demonstrates that 3D shape–selective neurons in the macaque inferior temporal cortex code the second spatial derivative of disparity. To what extent these neurons integrate binocular disparity with monocular depth cues will be the focus of future research.

Experimental Procedures

Subjects

Two male rhesus monkeys (J. and L.) participated in the experiments. Both were emmetropic and showed excellent stereopsis. Reliable stereoVEPs (Janssen et al., 1999a) were obtained with disparity steps of 0.06 deg. Horizontal and vertical movements of the right eye were recorded with the scleral search coil technique (Judge et al., 1980) at a sampling rate of 200 Hz. To measure possible vergence eye movements, monkey J. was implanted with a second coil in the left eye. The animals were trained to keep their gaze within 0.7 deg of a fixation target. After 1000 ms of stable fixation, the stimulus was presented for 800 ms. Only trials in which the monkey had maintained fixation for the entire duration of the trial were rewarded with juice and were included in the analysis.

Recording Sites

Standard extracellular recordings were made with tungsten microelectrodes in the anterior part of the lower bank of the STS (Janssen et al., 2000). The recording chamber was implanted stereotactically with reference to MR images (targeted Horsley-Clark coordinates: 16 mm anterior, 22 mm lateral). For monkey J., a CT scan obtained with the guiding tube in two positions that contained responsive neurons confirmed that the recording chamber was implanted at the targeted coordinates. In monkey L., the guiding tube position was visualized directly with a copper sulfate–filled glass pipette in the MRI. The validity of these reconstructions was verified in two other rhesus monkeys, in which this procedure was compared with histological verification of the recording positions.

Stimuli and Testing Procedure

The stimuli were disparity-defined 3D shapes filled with a texture of random dots. We imposed 4 pairs of depth profiles onto each of eight simple 2D shapes (e.g., a circle, an ellipse, or the shapes depicted in Figure 4). This procedure yielded a stimulus set consisting of 32 pairs of curved 3D shapes. The two members of a pair of 3D shapes utilize the same two monocular images (Janssen et al., 1999b). By interchanging the two monocular images presented to the right and left eyes, one creates two 3D shapes that differ only in the sign of their binocular disparity. Perceptually, however, the members of a pair differ dramatically, since concave surfaces become convex.

The stimuli were presented dichoptically by means of a double pair of ferroelectric liquid crystal shutters, which were placed in front of the monkeys' eyes. Each shutter closed and opened at a rate of 60 Hz, synchronized with the vertical retrace of the monitor (VRG digital multisync monitor with P46 ultrarapid decay phosphor). Stimulus luminance measured on the display equaled 43 cd/m^2, whereas measuring behind the shutters operating at 60 Hz, this value equaled 2.5 cd/m^2 (contrast $= 4 = \Delta I/I$). No signal was discernible behind the closed shutters using a photomultiplier 475R (Brandenburg, Surrey, UK) equipped with a Hamamatsu R453 tube (Hamamatsu). Therefore, the combination of a fast phosphor, a relatively low stimulus luminance, and a double pair of liquid crystal shutters eliminated the cross-talk between the monocular images entirely. The standard vertical dimension of the stimulus measured 5.6 deg (the horizontal dimension ranged from 5.6 to 4.5 deg), dot density was 50%, and dot size was 3.8 arcmin (2×2 pixels, 1 pixel $= 1.9$ arcmin). In the size test, the vertical dimension of the stimuli measured 8.4 deg, 5.6 deg, or 2.8 deg. A fixation target (diameter: 24 arcmin) was superimposed on the stimulus. The fixation distance was 86 cm. In each recording session, three different random dot textures were generated and used to fill each of the shapes. Presentation of shapes with different textures was interleaved.

Sine functions or a Gaussian function defined the variation of disparity over space. In addition, a subset of the neurons was tested with a quadratic function. To avoid texture density cues, disparity varied only along the vertical axis of the shape. First-order stimuli consisted of least-squares approximations of the upper or lower part of the 3D shape, which were extrapolated over the entire surface of the shape. The linear approximations of the original 3D shapes consisted of the connected least-squares approximations of the upper and lower parts of the shape (Figure 6B). Three or four different discrete approximations were used, each consisting of two or three segments separated by a disparity step equal to the disparity magnitude in the original 3D shape. The discrete stimuli consisting of three segments differed in the size of their central part (3.6, 1.8, or 0.9 deg), whereas one discrete stimulus consisted of two segments of equal size. In the size test, three quadratic functions defined the variation of disparity over the vertical axis. Each size was presented with each of the three quadratic functions. Therefore, there was no difference from size to size in the amount of disparity curvature in the stimuli.

We searched for responsive neurons using only one member of each 3D pair (four 3D profiles combined with eight 2D shapes, maximal disparity magnitude: 0.65 deg). A responsive neuron was then tested in detail by presenting two 3D pairs derived from a single 2D shape. One of the pairs included the 3D shape to which the neuron responded most strongly in the search test. Because most TE neurons include the fovea in their receptive field (Desimone and Gross, 1979), all stimuli were presented foveally (except in the frontoparallel position test) while the monkeys performed a fixation task. No attempt was made to optimize stimulus size. We determined the selectivity for disparity-defined 3D shapes by comparing the responses with the two members of a pair of 3D shapes. As a control, the monocular images of each 3D shape were presented to the left and right eyes separately. For the majority of the neurons, the sequence of tests, after 3D shape selectivity had been established, was as follows: position-in-depth test, sensitivity test, disparity order test, and frontoparallel position or size test. This procedure allowed us to adjust the disparity magnitude in the two final tests according to the response pattern in the sensitivity test.

Data Analysis and Tests

Net neural responses were computed trialwise by subtracting the number of spikes counted in a 400 ms interval immediately preceding stimulus onset from the number of spikes in a 400 ms interval starting 80 ms after stimulus onset. An ANOVA was used to test the significance of the 3D shape selectivity ($p < 0.05$) or responsiveness (split plot design; Kirk, 1968). To compare the responses with members of a pair of 3D shapes, we used a post hoc least significant difference test. 3D shape selectivity was judged not to arise from purely monocular mechanisms if the difference in response between the dichoptic presentations was at least three times the difference between the sum of the responses to the two monocular presentations (Janssen et al., 1999b).

In the position-in-depth test, the preferred and nonpreferred 3D shapes were presented at five different positions in depth, ranging from -0.5 deg (near) to $+0.5$ deg (far) disparity in equal steps. The selectivity index (SI_m) for the middle position in the position-in-depth test was defined as (response to the preferred 3D shape $-$ response

to the nonpreferred 3D shape)/(response to the preferred 3D shape + response to the nonpreferred 3D shape). The selectivity index for the worst position (SI_w) was defined as (smallest response to the preferred 3D shape − largest response to the nonpreferred 3D shape)/(smallest response to the preferred 3D shape + largest response to the nonpreferred 3D shape). To avoid spuriously large values of the selectivity index, the index was set to zero if both responses were smaller than 3 spikes/s. Indices larger than 1.5 were set to 1.5.

In the sensitivity test, preferred and nonpreferred 3D shapes (i.e., the two members of a pair of 3D shapes) were presented with six disparity magnitudes. The smallest magnitude tested (0.032 deg for concave and Gaussian, and 0.064 deg for tilted and sinusoidal, 3D shapes) was the smallest disparity variation (1 or 2 pixels) that could be generated given the resolution of the display and the fixation distance (86 cm). We classified the neurons into three categories. In broad band neurons, disparity magnitude showed no significant effect ($p > 0.05$) in an ANOVA comparing the six magnitudes of the preferred 3D shape, whereas magnitude did show a significant effect in tuned and monotonic neurons. Tuned neurons possessed an optimal disparity magnitude and a significant decline in response on either side of that optimum (post hoc least significant difference test, $p < 0.05$). For neurons tuned to small magnitudes, the response to the preferred 3D shape at the smallest magnitude was compared with the response elicited by the corresponding nonpreferred 3D shape. For monotonic neurons, the largest magnitude in the test evoked the largest response or a response statistically indistinguishable from the response to the second largest magnitude.

The disparity order test consisted of presentations of the original pair of 3D shapes, first-order stimuli, and linear and discrete approximations of the original 3D shapes. Neurons were classified into four groups. First-order neurons were equally selective for the first-order approximation or the original 3D shapes, as evidenced by the absence of a significant interaction between 3D structure (preferred versus nonpreferred) and stimulus type (original versus first-order). Second-order neurons were significantly more selective for the original 3D shapes than for the first-order stimuli (significant interaction between 3D structure and approximation). Within the second-order cells, discrete neurons were as selective for the discrete and linear approximations as for the original 3D shape: the interaction between stimulus type and approximation (original, linear, and discrete approximation) was not significant. Wedge neurons showed a significant interaction between stimulus type and approximation but no significant response difference between the original 3D shape and its linear approximation. Curvature neurons were distinguished from other second-order cells by a response to the original 3D shape significantly larger than that to its linear approximation (post hoc least significant difference test, $p < 0.05$).

Acknowledgments

This work was supported by the Geneeskundige Stichting Koningin Elisabeth, the Fonds voor Wetenschappelijk Onderzoek Vlaanderen, and grants GOA 95-99/06 and GOA 2000/11. P. J. is a research assistant and R. V. a research associate of the Fonds voor Wetenschappelijk Onderzoek Vlaanderen. We thank M. Depaep, P. Kayenbergh, G. Meulemens, G. Vanparrys, and W. Spileers.

Received February 24, 2000; revised June 5, 2000.

References

Baizer, J.S., Ungerleider, L.G., and Desimone, R. (1991). Organization of visual inputs to the inferior temporal and posterior parietal cortex in macaques. J. Neurosci. *11*, 168–190.

Burkhalter, A., and Van Essen, D.C. (1986). Processing of color, form and disparity information in visual areas VP and V2 of ventral extrastriate cortex in the macaque monkey. J. Neurosci. *6*, 2327–2351.

Cumming, B.G., and Parker, A.J. (1999). Binocular neurons in V1 of awake monkeys are selective for absolute, not relative, disparity. J. Neurosci. *19*, 5602–5618.

Dean, P. (1976). Effects of inferotemporal cortex lesions on the behaviour of monkeys. Psychol. Bull. *83*, 41–71.

Desimone, R., and Gross, C.G. (1979). Visual areas in the temporal cortex of the macaque. Brain Res. *178*, 363–380.

Desimone, R., Albright, T.D., Gross, C.G., and Bruce, C.J. (1984). Stimulus-selective properties of inferior temporal neurons in the macaque. J. Neurosci. *4*, 2051–2062.

Gatass, R., Sousa, A.P., and Gross, C.G. (1988). Visuotopic organization and extent of V3 and V4 of the macaque. J. Neurosci. *8*, 1831–1845.

Gross, C.G., Rocha-Miranda, C.E., and Bender, D.B. (1972). Visual properties of neurons in inferotemporal cortex of the macaque. J. Neurophysiol. *35*, 96–111.

Harwerth, R.S., and Boltz, R.L. (1979). Stereopsis in monkeys using random dot stereograms: the effect of viewing duration. Vision Res. *19*, 985–991.

Harwerth, R.S., Smith, E.L., and Siderov, J. (1995). Behavioral studies of local stereopsis and disparity vergence in monkeys. Vision Res. *35*, 1755–1770.

Howard, I.P., and Rogers, B.J. (1995). Binocular Vision and Stereopsis (New York: Oxford University Press).

Ito, M., Tamura, H., Fujita, I., and Tanaka, K. (1995). Size and position invariance of neuronal responses in monkey inferotemporal cortex. J. Neurophysiol. *73*, 218–226.

Iwai, E., and Mishkin, M. (1969). Further evidence on the locus of the visual area in the temporal lobe of the monkey. Exp. Neurol. *25*, 585–594.

Janssen, P., Vogels, R., and Orban, G.A. (1999a). Assessment of stereopsis in rhesus monkeys using visual evoked potentials. Doc. Ophthalmol. *95*, 247–255.

Janssen, P., Vogels, R., and Orban, G.A. (1999b). Macaque inferior temporal neurons are selective for disparity-defined 3D shape. Proc. Natl. Acad. Sci. USA *96*, 8217–8222.

Janssen, P., Vogels, R., and Orban, G.A. (2000). Selectivity for three-dimensional shape that reveals distinct areas in macaque inferior temporal cortex. Science *288*, 2054–2056.

Judge, S.J., Richmond, B.J., and Chu, F.C. (1980). Implantation of magnetic search coils for measurement of eye position: an improved method. Vision Res. *20*, 535–538.

Kirk, R.E. (1968). Experimental Design: Procedures for the Behavioral Sciences (Belmont, CA: Brooks-Cole).

Koenderink, J.J., and van Doorn, A.J. (1976). Geometry of binocular vision and a model for stereopsis. Biol. Cybern. *21*, 29–35.

Komatsu, H., Ideura, Y., Kaji, S., and Yamane, S. (1992). Color selectivity of neurons in the inferior temporal cortex of the awake macaque monkey. J. Neurosci. *12*, 408–424.

Lowe, D. (1986). Perceptual Organization and Three-Dimensional Shape Coding in Inferior Temporal Cortex Visual Recognition (Boston: Kluwer Academic).

Maunsell, J.H.R., and Van Essen, D.C. (1983). Functional properties of neurons in middle temporal visual area of the macaque monkey. II Binocular interactions and sensitivity to binocular disparity. J. Neurophysiol. *49*, 1148–1167.

Norman, J., Lappin, J.S., and Zucker, S.W. (1991). The discriminability of smooth stereoscopic surfaces. Perception *20*, 789–807.

Poggio, G.F., and Fischer, B. (1977). Binocular interaction and depth sensitivity in striate and prestriate cortex of behaving rhesus monkey. J. Neurophysiol. *40*, 1392–1405.

Poggio, G.F., Gonzalez, F., and Krause, F. (1988). Stereoscopic mechanisms in monkey visual cortex: binocular correlation and disparity selectivity. J. Neurosci. *8*, 4531–4550.

Prince, S.J.D., and Rogers, B.J. (1998). Sensitivity to disparity corrugations in peripheral vision. Vision Res. *38,* 2533–2537.

Rogers, B.J., and Cagenello, R. (1989). Disparity curvature and the perception of three-dimensional surfaces. Nature *339*, 135–137.

Roy, J.P., Komatsu, H., and Wurtz, R.H. (1992). Disparity sensitivity of neurons in monkey extrastriate area MST. J. Neurosci. *12*, 2478–2492.

Sary, G., Vogels, R., and Orban, G.A. (1993). Cue-invariant shape selectivity in inferior temporal cortex. Science *260*, 995–997.

Sato, T., Kawamura, T., and Iwai, E. (1980). Responsiveness of inferotemporal single units to visual pattern stimuli in monkeys performing discrimination. Exp. Brain Res. *38*, 313–319.

Schwartz, E.L., Desimone, R., Albright, T.D., and Gross, C.G. (1983). Shape recognition and inferior temporal neurons. Proc. Natl. Acad. Sci. USA *80*, 5776–5778.

Seltzer, B., and Pandya, D.N. (1978). Afferent cortical connections and architectonics of the superior temporal sulcus and surrounding cortex in the rhesus monkey. Brain Res. *149*, 1–24.

Shikata, E., Tanaka, Y., Nakamura, H., Taira, M., and Sakata, H. (1996). Selectivity of the parietal visual neurones in 3D orientation of surface of stereoscopic stimuli. Neuroreport *7*, 2389–2394.

Stevens, K.A., and Brookes, A. (1988). Integrating stereopsis with monocular interpretations of planar surfaces. Vision Res. *28*, 371–386.

Taira, M., Tsutsui, K.-I., Jiang, M., Yara, K., and Sakata, H. (2000). Parietal neurons represent surface orientation from the gradient of binocular disparity. J. Neurophysiol. *83*, 3140–3146.

Tanaka, K., Fukuda, H.K., and Moriya, Y. (1991). Coding visual images of objects in the inferotemporal cortex of the macaque monkey. J. Neurophysiol. *66*, 170–189.

Ungerleider, L.G., and Mishkin, M. (1982). Two cortical visual systems. In Analysis of Visual Behavior, D.J. Ingle et al., eds. (Cambridge, MA: MIT Press), pp. 549–586.

Vogels, R. (1999). Categorization of complex visual images by rhesus monkeys. II: Single-cell study. Eur. J. Neurosci. *11*, 1239–1255.

Weiskrantz, L., and Saunders, R.C. (1984). Impairments of visual object transforms in monkeys. Brain *107*, 1033–1072.